Prediction of Wind Turbine Rotor Loads Using the Beddoes-Leishman Model for Dynamic Stall

K. Pierce

A. C. Hansen

Mechanical Engineering Department,
University of Utah,
Salt Lake City, UT 84112

The Beddoes-Leishman model for unsteady aerodynamics and dynamic stall has recently been implemented in YawDyn, a rotor analysis code developed at the University of Utah for the study of yaw loads and motions of horizontal axis wind turbines. This paper presents results obtained from validation efforts for the Beddoes model. Comparisons of predicted aerodynamic force coefficients with wind tunnel data and data from the combined experiment rotor are presented. Also, yaw motion comparisons with the combined experiment rotor are presented. In general the comparisons with the measured data are good, indicating that the model is appropriate for the conditions encountered by wind turbines.

Introduction

Previous work has shown the importance of including dynamic stall in the prediction of wind turbine rotor loads. Predictions of Combined Experiment Rotor (CER) loads were improved by the addition of the Gormont dynamic stall model in YawDyn, a horizontal axis wind turbine analysis code developed at the University of Utah (Hansen et al., 1990; Hansen, 1992). Also, dynamic stall events are evident in the airfoil pressure data obtained from operating wind turbines (Hansen and Butterfield, 1993; Butterfield et al., 1991).

The Beddoes model was added to YawDyn after shortcomings were observed in the Gormont model. Hansen found that coefficients in the Gormont model needed to be modified to reproduce observed CER airfoil lift curves and yaw moments. This model also required a filter on the angle of attack to stabilize the lift coefficient prediction. The Beddoes model was added to YawDyn in hopes that it would be more applicable to the environment encountered by, and airfoils used in, wind turbines.

This paper presents results from validation efforts for the Beddoes model. Comparisons of predicted aerodynamic force coefficients with wind tunnel data as well as with full-scale operating wind turbine data are presented. Also, YawDyn predicted free-yaw motion of the CER are compared with measurements.

The Beddoes-Leishman Model

A detailed description of the model is given by Leishman and Beddoes (1986, 1989). For this paper a brief description seems appropriate, and is given below.

The Beddoes-Leishman model is semi-empirical. It is based on airfoil indicial response, and requires only steady two-dimensional data for implementation.

The airfoil attached flow response to a general angle of attack history is calculated from the superposition of individual indicial responses for each step. This attached flow response is then modified based upon the unsteady separation point. The separation point is given by $f = x/c$, where x is the point of flow separation measured from the trailing edge, and c is the airfoil chord length. An approximation to Kirchoff flow (Thwaites, 1960) relating the normal force to the separation point is given as

$$C_N = C_{N\alpha}(\alpha - \alpha_0)\left(\frac{1 + \sqrt{f}}{2}\right)^2, \tag{1}$$

where $C_{N\alpha}$ is the normal force curve slope, α is the angle of attack, α_0 is the zero-lift angle of attack, and f is the separation point.

A vortex lift contribution is also added when the conditions for vortex generation and vortex travel are present.

The Beddoes model accounts for the fact that the flow about the airfoil cannot change instantaneously, which is the cause of the dynamic events. The indicial response calculation requires finite time for the circulation about the airfoil to build or decay. An empirically derived time lag is associated with the movement of the separation point, and empirically derived time constants are associated with the growth and decay of the vortex lift.

This is in contrast to the Gormont model which calculates the lift coefficient based upon airfoil characteristics and the current time rate of change of angle of attack ($\dot{\alpha}$), and may therefore respond instantaneously to changes in $\dot{\alpha}$.

Model Modifications

Some minor modifications to the model were needed to make it applicable to the wind turbine environment and airfoils. Beddoes considers angles of attack from approximately $-10°$ to 30°, however wind turbines often operate outside of this range. The operating environment of the wind turbine requires that the model be capable of producing force coefficients through the full range of angle of attack from +180 deg to −180 deg. To accomplish this the angle of attack was modified as follows:

$$\text{for } |\alpha| \le 90 \text{ deg} \quad \alpha_m = \alpha$$

$$\alpha > 90 \text{ deg} \quad \alpha_m = 180 \text{ deg} - \alpha$$

$$\alpha < -90 \text{ deg} \quad \alpha_m = -180 \text{ deg} - \alpha \tag{2}$$

Where α is the current angle of attack and α_m is the modified angle of attack.

Contributed by the Solar Energy Division of THE AMERICAN SOCIETY OF MECHANICAL ENGINEERS for publication in the ASME JOURNAL OF SOLAR ENERGY ENGINEERING. Manuscript received by the ASME Solar Energy Division, Mar. 1994; final revision, Mar. 1995. Associate Technical Editor: P. S. Veers.

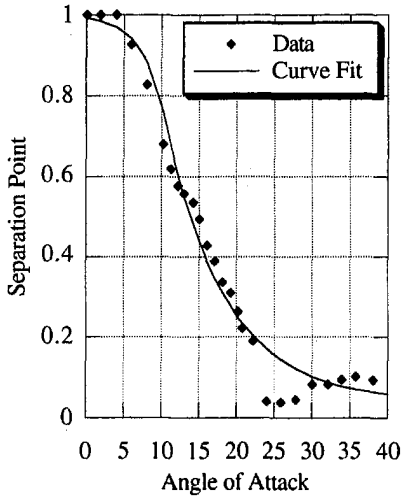

Fig. 1 Exponential curve fit to calculated separation point data, for a NACA 4415 at Re = 1.0 *M*

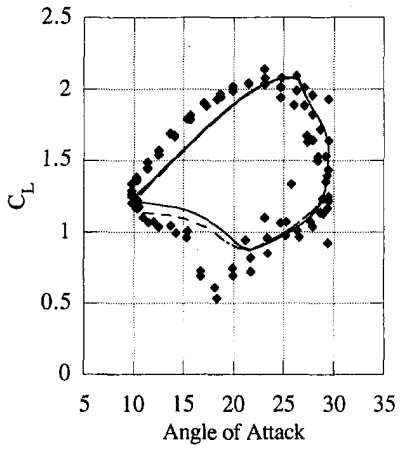

Fig. 3 NACA 4415 lift coefficient versus angle of attack. High amplitude oscillation. α = 19.7 + 9.8 sin (ωt), k = .096, M = .1

This represents the fact that the normal force is somewhat symmetric about +90 deg and −90 deg. This modified angle of attack is used for calculation of the separation point from the Kirchoff equation as well as for runtime calculation of the attached flow response. While the accuracy of the model for these high angles of attack is not known, due to the lack of test data, the results obtained are at least reasonable.

Beddoes uses an exponential curve fit to the airfoil separation point calculated using Eq. (1) and shown in Fig. 1. However, this did not work well with some of the airfoils tested. As can be seen in Fig. 2 below, some important features are lost when regenerating the normal force versus angle of attack curve using the exponential curve fit representation of the separation point. For this reason a lookup table was used, in which the calculated separation point values are stored with angle of attack values. Linear interpolation is used between points. This method is more applicable to all airfoils and accurately reproduces the normal force curve.

Beddoes also includes an empirical separation point shift for the "deep stall regime." However, whether or not this shifting increases or decreases, accuracy depends on the amplitude of oscillation of the airfoil. For high-amplitude oscillations increased accuracy was obtained by including the shift. However, for low-amplitude oscillations better accuracy was obtained without the shift. Also, the shifting was found to cause discontinuities and hence numerical instabilities in YawDyn force calculations for very small angle of attack oscillation amplitudes. For these reasons the shifting has been removed from the model used in YawDyn. This shifting will be discussed further below.

Two-Dimensional Wind Tunnel Simulations

While the flow encountered by wind turbines is far from two-dimensional, it is necessary for the method to accurately represent two-dimensional wind tunnel data if there is to be any hope of representing the complex flow encountered by wind turbines.

Figures 3 through 6 are comparisons between predicted and measured lift and drag curves for a NACA 4415. The conditions for the comparisons are given in the figures, where α is the angle of attack, ω is the circular frequency, k is the reduced frequency given by $k = \omega c/2V$, and M is the mach number. The data was provided by Ohio State University (Gregorek and Reuss, 1992). Also included in these figures are the effects of the previously mentioned separation point shift. Figures 3 and 4 are comparisons for high-amplitude oscillation. The shifting in this case improves normal force coefficient predictions slightly by delaying flow reattachment. There is little effect on the drag curve. Figures 5 and 6 are for low amplitude oscillation where the effects of the shift are more pronounced. For the lower amplitude case the model including the shift over estimates the

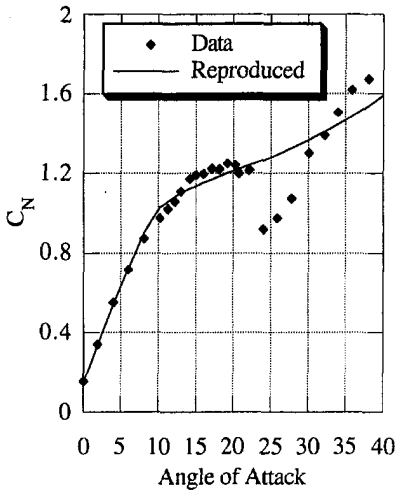

Fig. 2 Comparison between data and reproduced curve using exponential curve fit to separation point

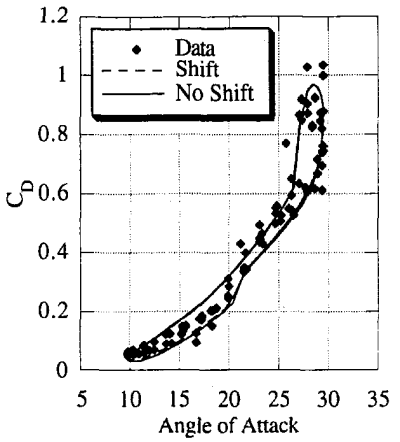

Fig. 4 Drag coefficient versus angle of attack. Test conditions as given in Fig. 3

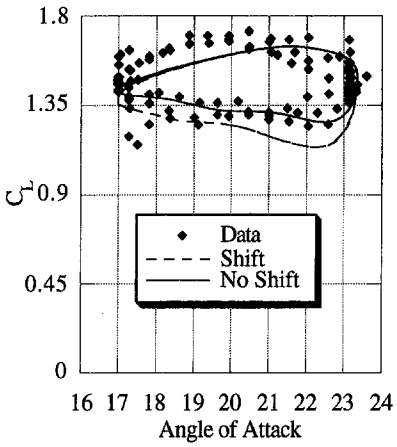

Fig. 5 NACA 4415 lift coefficient versus angle of attack. Low amplitude oscillation. $\alpha = 20.2 + 3.2 \sin(\omega t)$, $k = .087$, $M = .1$

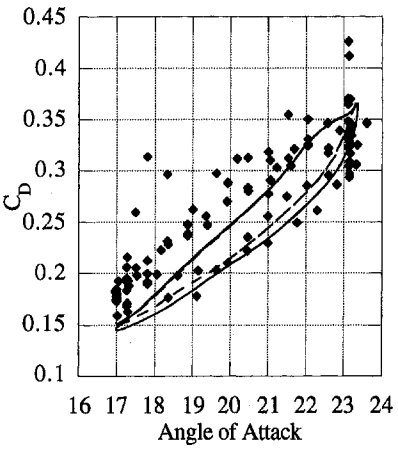

Fig. 6 Drag coefficient versus angle of attack. Test conditions as given in Fig. 5

amount of airfoil stall. Also the drag comparison is improved somewhat by the elimination of the shifting.

These figures show the modified Beddoes model reproduces quite accurately the qualitative and quantitative features of dynamic stall.

Comparisons to CER Data

Figure 7 is a plot of yaw angle versus time, as predicted by YawDyn compared to measured data. Wind speed, direction, vertical wind, and vertical and horizontal shears, all calculated from the Combined Experiment vertical plane array of anemometers, were used as inputs to YawDyn. As can be seen in the figure the YawDyn comparison with the data is very good, and captures all of the features seen in the data. While the yaw angle is well represented by YawDyn and the normal force coefficient predicted by YawDyn captures the mean quite accurately, the predicted normal force coefficient lacks the higher frequency components observed in the data, as seen in Fig. 8. This is possibly due to the way in which the measured wind is processed for input to YawDyn. However, for other design codes, or if higher frequency wind data are used in YawDyn, these higher frequency components may be present, and the aerodynamic model used in these codes should be capable of representing the aerodynamic force coefficients for these higher frequencies.

To determine if the Beddoes model was applicable to these higher frequencies, the angle of attack measured from the CER was used as input to the Beddoes subroutines. This permitted examination of only the angle of attack-normal force coefficient relationship, eliminating all rotor dynamics and wind input. Figure 8 is a plot of normal force coefficient versus time. Shown in this figure are the normal force coefficient values measured from the CER, the values predicted by YawDyn using the measured wind, and the values predicted using the measured angle of attack from the CER as input to the Beddoes subroutines, labeled in the figure as "simulated". The simulated curve follows the measured data quite accurately, indicating that the method is capable of accurate normal force predictions for these higher frequencies. It also indirectly indicates that the angle of attack measurement at the outboard stations is quite accurate.

After obtaining good predictions at the outboard blade station, comparisons were then made for the inboard (30 percent) station. The blades of the combined experiment rotor are untwisted, producing much higher angles of attack at the inboard stations. The initial comparisons are shown in Fig. 9. The predicted mean values are much lower than those observed in the data, and in general the comparisons are not very good. To determine why the model predictions were inaccurate at the inboard station, the measured data were studied more closely.

One cause of discrepancy is that at the inboard station the airfoil did not stall as predicted by the static two-dimensional data. This is shown in Fig. 10, notice the measured data stay well above the static line. This is due to the delayed static stall which has been observed by others (Butterfield, 1991). In an attempt to model this delayed static stall the static curve was modified to pass through the measured data, as thought to be appropriate. This produced the curve labeled as "modified" in Fig. 10.

Also, upon closer examination of the measured angle of attack, the angle of attack indicator, which is of the vane type, was seen to "ring" after the blade passed through the tower shadow. This is shown in Fig. 11, where the YawDyn angle of attack prediction is included only to show that the "ringing" does occur after passing through the tower shadow (0 deg azimuth). Although the ringing was less pronounced at other times in the data, the accuracy of the angle of attack indicator is questionable at this inner station.

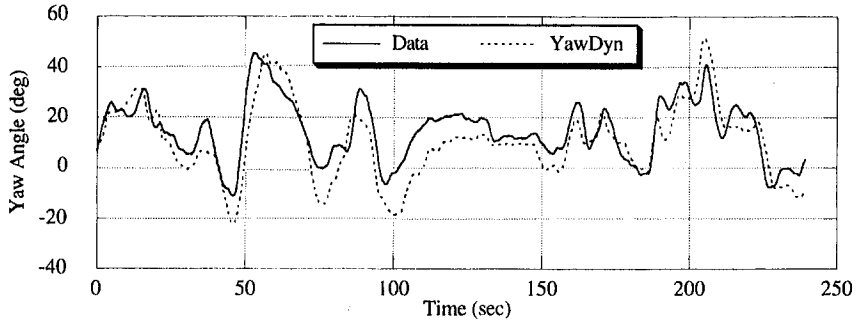

Fig. 7 YawDyn prediction of yaw angle for the CER with a mean wind velocity of 12 m/s, 72 rpm

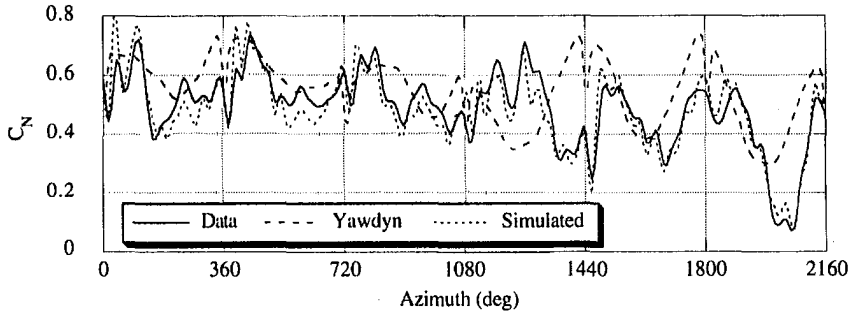

Fig. 8 80 percent radius normal force coefficient comparison. Conditions as given in Fig. 7

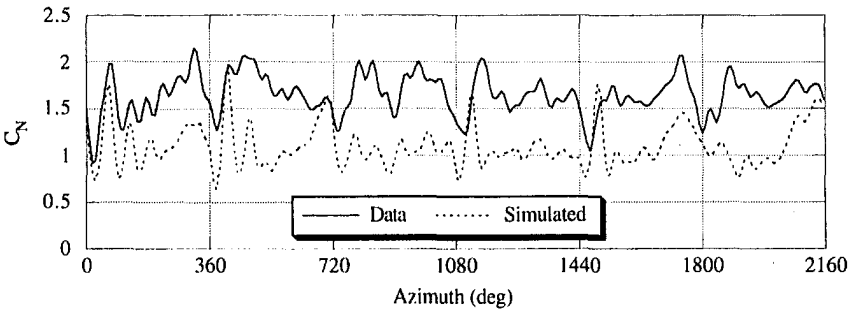

Fig. 9 Initial prediction of normal force coefficient at the 30 percent station. Conditions as given in Fig. 7

However, there was no obvious way to eliminate this ringing from the data. Therefore the inboard simulation was performed again using the modified static curve, and the measured angle of attack. The results of this simulation are shown in Fig. 12. The mean value now matches the data quite closely, and many of the features of the data are now represented. Thus it appears that the inboard normal force coefficient can be predicted quite accurately if the static lift curve is modified to account for the delay in stall. Methods for estimating the static lift curve of a rotating blade are the subject of current research (Eggers and Digumarthi, 1992). However, it is encouraging that the dynamic character is well represented when the static lift curve is known.

It is of interest to note in Fig. 12 that the measured normal force coefficient oscillates at the same high frequency seen in the measured angle of attack (AOA). This indicates that the AOA sensor may be responding to actual fluctuations in AOA rather than simply "ringing" after the tower shadow impulse as previously suspected. It does appear that the sensor's dynamic response exaggerates the AOA response, as the oscillations in normal coefficient are smaller than those in AOA. No explanation for this observation can be given at this time, and is mentioned only as a point of interest for future investigation.

Conclusions

In general the comparisons between the aerodynamic force coefficients predicted by the Beddoes method and measured

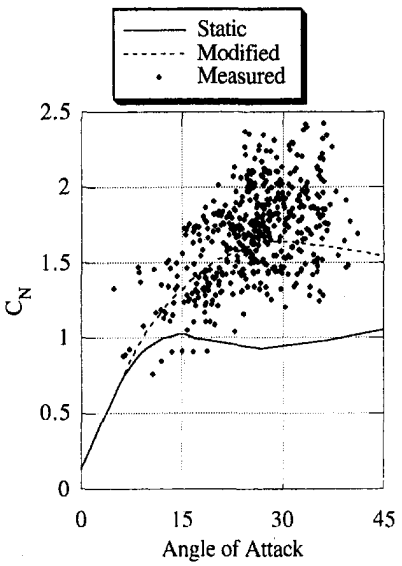

Fig. 10 Comparison between static normal force curve and data points measured at the 30 percent station

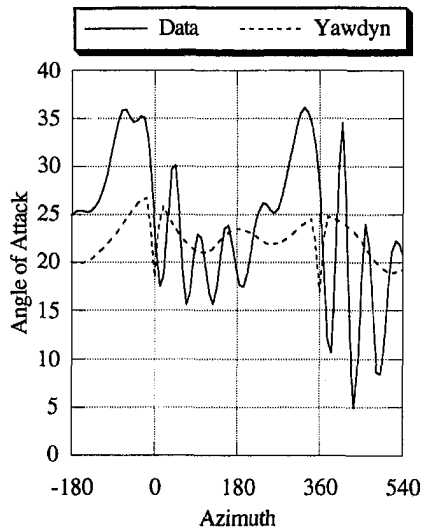

Fig. 11 Illustration of ringing of vane-type angle of attack indicator

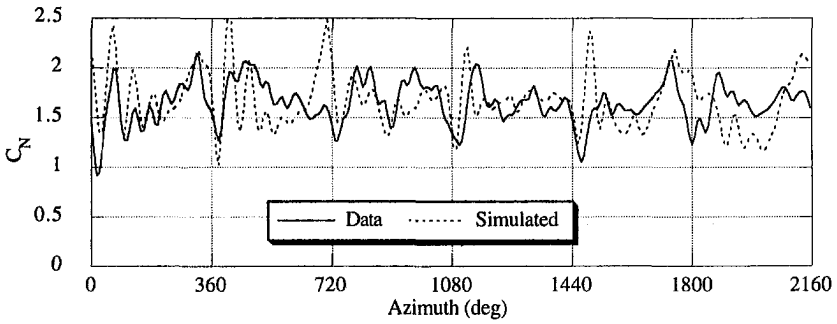

Fig. 12 Comparison between predicted and measured normal force coefficients using modified static curve. Conditions as given in Fig. 7

values are very good. In comparisons with two-dimensional unsteady wind tunnel data the Beddoes model reproduces the measured data quite accurately. Also for the CER 80 percent station, measured normal force coefficients are accurately predicted by the Beddoes method when using the measured angle of attack. This indicates that the model is appropriate for the operating conditions encountered by wind turbines.

At inboard stations the Beddoes model is capable of representing the dynamic behavior when the static lift curve of the rotating blade is known. In the absence of test data, the best method for determining this effective static curve is unknown.

YawDyn predictions of the yaw motion of the CER are surprisingly good, and capture all of the features seen in the test data.

Acknowledgments

This research has been supported by the National Renewable Energy Laboratory to provide aerodynamic subroutines for use in rotor design and analysis codes.

References

Butterfield, C. P., Huyer, S., and Simms, D., 1991, "Recent Results from Data Analysis of Dynamic Stall on Wind Turbine Blades," Natl. Renewable Energy Lab., NREL Tech. Rep. 257–4654.

Eggers, A. J., and Digumarthi, R. V., 1992, "Approximate Scaling of Rotational Effects of Mean Aerodynamic Moments and Power Generated By the Combined Experiment Rotor Blades Operating in Deep-Stalled Flow," *11th ASME Wind Energy Symposium,* pp. 33–43.

Gormont, R. E., 1973, "A Mathematical model of Unsteady Aerodynamics and Radial Flow for Application to Helicopter Rotors," U. S. Army Air Mobility Research and Development Laboratory, USAAMRDL Technical Report, 76-67.

Gregorek, G. M., and Reuss, R. L., 1992 personal communication.

Hansen, A. C., Butterfield, C. P., and Cui, X., 1990, "Yaw Loads and Motions of a Horizontal Axis Wind Turbine," ASME JOURNAL OF SOLAR ENERGY ENGINEERING, Vol. 112, pp. 310–314.

Hansen, A. C., 1992, "Yaw Dynamics of Horizontal Axis Wind Turbines: Final Report," Natl. Renewable Energy Lab., NREL Tech. Rep. 442–4822.

Hansen, A. C., and Butterfield, C. P., 1993, "Aerodynamics of Horizontal-Axis Wind Turbines," *Annual Rev. Fluid Mech.,* Vol. 25, pp. 115–149.

Leishman, J. G., and Beddoes, T. S., 1986, "A Generalized Model For Airfoil Unsteady Behavior and Dynamic Stall Using the Indicial Method," *Proceedings of the 42nd Annual forum of the American Helicopter Society,* Washington D. C., pp. 243–266.

Leishman, J. G., and Beddoes, T. S., 1989, "A Semi-Empirical Model for Dynamic Stall," *Journal of the American Helicopter Society,* Vol. 34, No. 3, pp. 3–17.

Leishman, J. G., 1989, "Modeling Sweep Effects on Dynamic Stall," *Journal of the American Helicopter Society,* Vol. 34, No. 3, pp. 18–29.

McCroskey, W. J., 1981, "The Phenomenon of Dynamic Stall," NASA Technical Memorandum, TM81264.

Thwaites, B., ed., 1960, *Incompressible Aerodynamics,* Oxford University Press, New York, pp. 168–170.

Wind Energy Program, 1992, "NREL/DOE Combined Experiment Topic Reports from Phase I and Phase II Testing," Natl. Renewable Energy Lab., compiled Jan. 1992.